Mon. Not. R. Astron. Soc. **423,** 284–293 (2012) doi:10.1111/j.1365-2966.2012.20871.x

A new observational tracer for high-density disc-like structures around B[e] supergiants⋆

A. Aret,[1,2]† M. Kraus,[1]† M. F. Muratore[3,4]† and M. Borges Fernandes[5]†

[1]*Astronomický ústav, Akademie věd České republiky, Fričova 298, 251 65 Ondřejov, Czech Republic*
[2]*Tartu Observatory, 61602, Tõravere, Tartumaa, Estonia*
[3]*Departamento de Espectroscopía Estelar, Facultad de Ciencias Astronómicas y Geofísicas, Universidad Nacional de La Plata, Paseo del Bosque s/n, B1900FWA, La Plata, Argentina*
[4]*Instituto de Astrofísica de La Plata, CCT La Plata, CONICET-UNLP, Paseo del Bosque s/n, B1900FWA, La Plata, Argentina*
[5]*Observatório Nacional, Rua General José Cristino 77, 20921-400 São Cristovão, Rio de Janeiro, Brazil*

Accepted 2012 March 2. Received 2012 March 2; in original form 2011 December 13

ABSTRACT

The disc formation mechanism of B[e] supergiants is one of the puzzling phenomena in massive star evolution. Rapid stellar rotation seems to play an important role for the non-spherically symmetric mass-loss leading to a high-density disc- or ring-like structure of neutral material around these massive and luminous objects. The radial density and temperature structure as well as the kinematics within this high-density material are, however, not well studied. Based on the high-resolution optical spectra of a sample of B[e] supergiants in the Magellanic Clouds we especially searched for tracers of the kinematics within their discs. Besides the well-known [O I] lines, we discovered the [Ca II] λλ7291, 7324 lines which can be used as a complementary set of disc tracers. We find that these lines originate from very high density regions, located closer to the star than the [O I] λ5577 line-forming region. The line profiles of both the [O I] and the [Ca II] lines indicate that the discs or rings of high-density material are in Keplerian rotation. We estimate plausible ranges of disc inclination angles for the sample of B[e] supergiants and suggest that the star LHA 120-S 22 might have a spiral arm rather than a disc.

Key words: circumstellar matter – stars: emission line, Be – supergiants – stars: winds, outflows.

1 INTRODUCTION

B[e] supergiants (B[e]SGs) are evolved massive stars with a large amount of circumstellar material in the form of atomic and molecular gas as well as dust. The presence of gas is indicated by the numerous emission lines from both forbidden and permitted transitions of atoms in different ionization stages. Molecular emission has been reported for many B[e]SGs: TiO emission has been detected at optical wavelengths (Zickgraf et al. 1989; Torres et al., in preparation) and CO emission has been observed in the near-infrared (McGregor, Hillier & Hyland 1988; Morris et al. 1996; Liermann et al. 2010; Muratore et al. 2010). The presence of dust is obvious from the strong infrared excess emission in the photometric and spectroscopic data (e.g. Zickgraf et al. 1986; Bonanos et al. 2009, 2010), and the composition of this dust shows indications for both oxygen (crystalline silicates) and carbon (polycyclic aromatic hydrocarbons) chemistry (Kastner et al. 2010).

The co-existence of a normal B-supergiant radiation-driven wind and a large amount of molecular and dusty material suggests that the geometry of the circumstellar material cannot be spherically symmetric, and polarimetric studies of B[e]SGs in the Magellanic Clouds (e.g. Magalhães 1992; Melgarejo et al. 2001; Magalhães et al. 2006) and of Galactic B[e] stars and B[e]SG candidates (Oudmaijer & Drew 1999) supported a flat, disc-like geometry. Though studied for many decades, the structure and geometry, as well as the formation history of the B[e]SG discs, still remain unknown.

Zickgraf et al. (1985) suggested that the discs are formed by a slow, high-density equatorial outflow. Such an equatorially outflowing disc could result from rapid stellar rotation via the bistability mechanism (Lamers & Pauldrach 1991; Pelupessy, Lamers & Vink 2000) or from the newly found slow-wind solutions (Curé 2004; Curé, Rial & Cidale 2005) that produce a slow but high-density wind in the equatorial region. Rapid stellar rotation could also be the reason for recombination of the ionized wind material in the equatorial plane (e.g. Kraus 2006), resulting in a large amount of neutral hydrogen close to the stellar surface, as was recently found

⋆Based on observations collected with the ESO 2.2 m telescope in La Silla, Chile, under programme 076.D-0609(A).

†E-mail: aret@aai.ee (AA); kraus@sunstel.asu.cas.cz (MK); fmuratore@carina.fcaglp.unlp.edu.ar (MFM); borges@on.br (MBF)

Table 1. Parameters of the observed B[e]SGs.

Object	Sp. type	$E(B-V)$	$T_{\rm eff}$ (10^3 K)	L (10^5 $L_\odot$)	Orientation	References
			SMC			
LHA 115-S 18	B0	0.40	25	3-4.6	±Pole-on	(1)
LHA 115-S 65	B2–3	0.15–0.20	17	5.0	Edge-on	(2)
			LMC			
LHA 120-S 12	B0.5	0.20–0.25	23	2.2	Intermediate	(2)
LHA 120-S 22	B0–B0.5	0.25–0.30	23–26	6–9.5	Edge-on	(2)
LHA 120-S 73	B8	0.12	12	2.9	±Pole-on	(2)
LHA 120-S 111	–	0.28	15.5	11.2	–	(4)
LHA 120-S 127	B0.5	0.25	22.5	13	Pole-on	(3)
LHA 120-S 134	B0	0.20–0.25	26	7.9	Pole-on	(2)

References: (1) Zickgraf et al. (1989); (2) Zickgraf et al. (1986); (3) Zickgraf et al. (1985); (4) McGregor et al. (1988).

for some B[e] stars and B[e]SGs (Kraus & Borges Fernandes 2005; Kraus, Borges Fernandes & de Araújo 2007, 2010).

However, for some individual B[e]SGs recent detailed investigations revealed that the simple outflowing-disc scenario does not hold. The set of [O I] λλ5577, 6300 lines trace physically distinct regions within the inner parts of the massive disc or ring which are so dense that hydrogen is already predominantly neutral (Kraus et al. 2007, 2010). On the other hand, information on the density, temperature and kinematics within the molecular parts of the disc can be obtained from the strength and structure of the CO first-overtone bands (e.g. Carr et al. 1993; Chandler et al. 1993; Carr 1995; Najita et al. 1996; Kraus et al. 2000; Liermann et al. 2010; Muratore et al. 2010). The fluxes, temperatures and kinematics obtained from these emissions hint towards the presence of a detached ring (or a detached disc-like structure) rather than a disc structure formed from a steady outflow (Kraus et al. 2010; Liermann et al. 2010; Muratore et al. 2010).

To study the formation mechanisms of B[e]SG discs it is important to combine the information on density, temperature and especially kinematics obtained from different sources, like optical emission lines and infrared molecular bands that trace different regions within the circumstellar material. The forbidden emission lines play a very important role in this study, because they are optically thin (e.g. Osterbrock 1989) and hence ideal tracers for density and temperature (see e.g. Kraus et al. 2005), and their profiles contain the full kinematical information of their formation region (Ignace & Brimeyer 2006; Kraus et al. 2010). However, most forbidden emission lines are formed in the low-density regions. The chance to find forbidden lines originating from the high-density disc complementing the well-known set of [O I] lines is rather low. Also, high-quality optical and near-infrared observations for most of the B[e]SGs are still lacking.

To overcome the difficulties in studying the structure and formation history of the B[e]SG discs we started an observational campaign focused on the search for typical density and velocity tracers in the spectra of these stars. Here we report on our results based on high-resolution optical spectra obtained for a total of eight B[e]SGs in the Magellanic Clouds. In these spectra we discovered, besides the well-known [O I] lines, a set of forbidden emission lines, the [Ca II] λλ7291, 7324 lines, as a new, valuable disc tracer.

2 OBSERVATION AND REDUCTION

Our sample consists of two B[e]SGs from the Small Magellanic Cloud and six from the Large Magellanic Cloud (SMC and LMC, respectively). The objects are listed in Table 1 together with the stellar parameters and possible disc orientations as found in the literature.

The observations were carried out on two consecutive nights, on 2005 December 10 and 11. We obtained high-resolution optical spectra using the Fibre-fed Extended Range Optical Spectrograph (FEROS) attached to the 2.2-m telescope at the European Southern Observatory (ESO) in La Silla (Chile).

FEROS is a bench-mounted echelle spectrograph with two fibres, each of them covering a circular sky area of 2 arcsec in diameter. The wavelength coverage extends from 3600 to 9200 Å and the spectral resolution is $R = 55\,000$ (in the region around 6000 Å). We made our own data reduction, since the pipeline presented some problems during that mission. Based on this, we used available MIDAS routines (Verschueren et al. 1997), including some modifications related to the FEROS characteristics. Thus, our data are reduced differentially relative to a master stellar and flat-field frame, considering the usual steps for echelle data reduction with the proper location and merge of the spectral orders. The spectra are rebinned taking into account the natural resolution of the detector. The telluric and barycentric velocity corrections have also been performed. From the sky lines we measured the accuracy of the wavelength calibration, which is better than 0.5 km s^{-1}.

To identify and delete cosmic rays from the spectra, we took a minimum of two spectra per star. The spectral lines did not show any variability in the individual exposures, so we added them up to achieve a better signal-to-noise ratio (S/N). Exposure times together with the final achieved S/N are listed in Table 2. The stellar radial velocities obtained from the central wavelength of the [O I] λ6300 line are also given in that table.

3 RESULTS

The FEROS spectra of the B[e]SGs display a large number of emission lines from permitted and forbidden transitions. Emission lines

Table 2. Exposure times (number of exposures is given in parentheses) and S/N at 5500 Å. The radial velocities V_r were derived using the [O I] λ 6300.

Object	Exposure (s)	Total S/N	V_r (km s^{-1})
LHA 115-S 18	1800 (2)	50	146
–	900 (1)	–	–
LHA 115-S 65	900 (2)	55	189
LHA 120-S 12	900 (2)	60	290
LHA 120-S 22	900 (2)	70	289
LHA 120-S 73	600 (1)	100	261
–	900 (1)	–	–
LHA 120-S 111	900 (2)	80	267
LHA 120-S 127	450 (2)	50	259
LHA 120-S 134	1800 (1)	70	267
–	900 (1)	–	–

from the latter are especially valuable, because forbidden lines are optically thin, and their profiles reflect the kinematics within their formation region. One interesting set of lines has been identified as the forbidden emission lines of neutral oxygen, [O I] λλ5577, 6300, 6364. While the two lines λλ6300, 6364 arise from the same upper energy level and hence are formed in the same region within the disc, the [O I] λ5577 line emerges from regions of higher density (for details see Kraus et al. 2007, 2010), i.e. from distances very close to the star. The ratio [O I] λ6300/λ5577 serves as an ideal indicator for temperature, density and ionization fraction of the disc material (Kraus et al. 2007, 2010). Since the emission of these two individual lines arises from physically distinct disc regions, i.e. regions with different velocities, their line fluxes and profiles deliver complementary information. This makes these two lines a valuable tool in the study of both the structure and kinematics of the discs, as was recently shown by Kraus et al. (2010) for the B[e]SG LHA 115-S 65 in the SMC.

Unfortunately, for many stars of our sample the [O I] λ5577 line is quite weak or even absent (see Figs 1 and 2). In addition, the S/N of the observed spectra in the wavelength region of this line is rather low (see Table 2). This hampers severely a proper determination of the physical parameters of their discs and emphasizes the need for additional lines that are capable of tracing the disc properties at different distances from the star.

Upon inspection of the FEROS spectra we found that all our B[e]SGs display strong line emission from the Ca II λλ8498, 8542, 8662 infrared triplet. Examples of the FEROS spectra around these lines are shown in Fig. 3 for three stars of our sample with different Ca II line profiles and different strengths in the adjacent hydrogen lines of the Paschen series. This emission is known to arise from high-density regions, and circumstellar discs are especially favoured locations. Emission in the Ca II infrared triplet has been reported for a diversity of objects: T Tauri stars (e.g. Hamann & Persson 1992a; Kwan & Fischer 2011), Herbig Ae/Be stars (e.g. Hamann & Persson 1992b), classical Be stars (e.g. Polidan & Peters 1976; Briot 1981; Andrillat, Jaschek & Jaschek 1988, 1990; Jaschek et al. 1988) and other, non-supergiant B[e] stars (Borges Fernandes et al. 2001, 2009).

Furthermore, we discovered strong line emission in [Ca II] λλ7291, 7324 in all our objects. So far, the appearance of these forbidden emission lines has been reported for only a few other disc sources (Hamann 1994; Hartigan, Edwards & Pierson 2004). Nevertheless, the detection of these forbidden lines is of particular interest, because the energy levels from which the [Ca II] lines emerge are coupled to those from which the Ca II infrared triplet lines arise. The presence or absence of the [Ca II] lines could thus be a suitable tracer for specific temperature and density conditions within the disc or wind.

In Figs 1 and 2 we plot the line profiles of the calcium lines together with those of the [O I] lines and of Hα. To compare widths and shapes of lines from different stars we plotted identical lines on the same radial velocity scale. Stellar radial velocities as listed in Table 2 have been subtracted. The close vicinity of the Ca II infrared triplet lines to adjacent Paschen lines could result in line blending. The distances of the individual Paschen lines Pa(16) λ8502, Pa(15) λ8545 and Pa(13) λ8665 from the Ca II lines are +157.7, +115.5 and +99.7 km s^{-1}, respectively. However, in the high-resolution FEROS spectra the shape of the Ca II lines is not distorted by the Paschen lines for most of our stars (see Figs 1, 2 and 3). One exception is LHA 120-S 22, in which the Paschen lines are extremely strong.

3.1 Line profile diversity

The appearance of the optical spectra of the B[e]SGs has been described in detail in the literature (e.g. Zickgraf et al. 1985, 1986, 1989). However, former observations were limited to wavelengths shorter than 7000 Å. This is the reason why the strong emission in both the Ca II infrared triplet and the forbidden [Ca II] lines was not reported earlier. Hence, we refrain from repeating a detailed spectral description, and instead we focus on these newly detected emission lines and discuss their shape with respect to the [O I] lines.

The different line widths of the forbidden lines are expected to reflect the kinematics of physically distinct regions. We note an increase in line width starting with the [O I] λλ6300, 6364 lines, through the [O I] λ5577 line, to the [Ca II] λλ7291, 7324 lines for all stars but LHA 120-S 127. In addition, we note a simultaneous change in the line profile. If the [O I] λλ6300, 6364 lines have a single-peaked, Gaussian shape, the [Ca II] λλ7291, 7324 lines show slight indications for double peaks. If the [O I] λλ6300, 6364 lines show slightly double-peaked profiles, the [Ca II] λλ7291, 7324 lines are wide and clearly doubly peaked. The width and shape of the [O I] λ5577 line are intermediate. However, a clear classification of its profile shape is difficult for most of our objects, because this line is usually weak and noisy. The profile shapes and the measured (if possible) peak separations in velocities are listed in Table 3.

The lines of the Ca II infrared triplet are always (much) broader than the forbidden emission lines, and their profiles show a diversity ranging from double (Fig. 1) to multiple peaked (Fig. 2). Where possible, the peak separations in velocities have been measured and are listed in Table 4. The double-peaked profiles of these lines, however, do not resemble those structures that refer to the formation within a rotating or equatorially outflowing medium as seems to be the case for the forbidden lines. Instead, they probably stem from absorption within a high-density medium.

The emission in the Hα line is the most prominent feature in all our spectra. Its strength ranges from about 25 to about 250 times the continuum flux. Its profile can be single peaked, double peaked or of P Cygni type. Its wings extend for all objects to large velocities. These high velocities, however, do not reflect real kinematics but are most probably caused by electron scattering in a high-density wind or disc.

3.2 Disc structure and kinematics

The obvious diversity we see in the line profiles indicates that the formation regions for different lines must be physically distinct. This

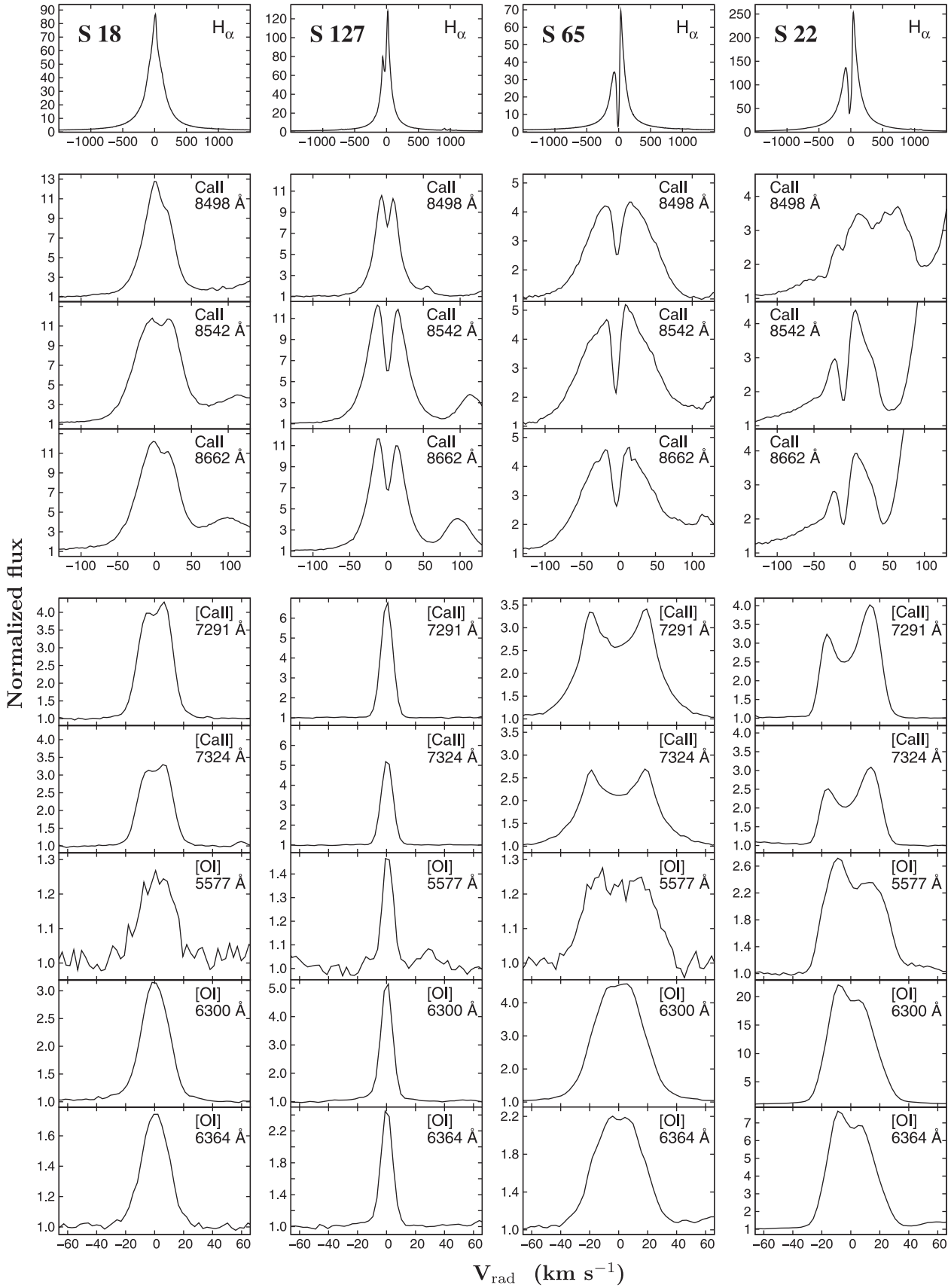

Figure 1. Line profile variety of stars seen pole-on (S 18, S 127) and edge-on (S 65, S 22). For details see the text.

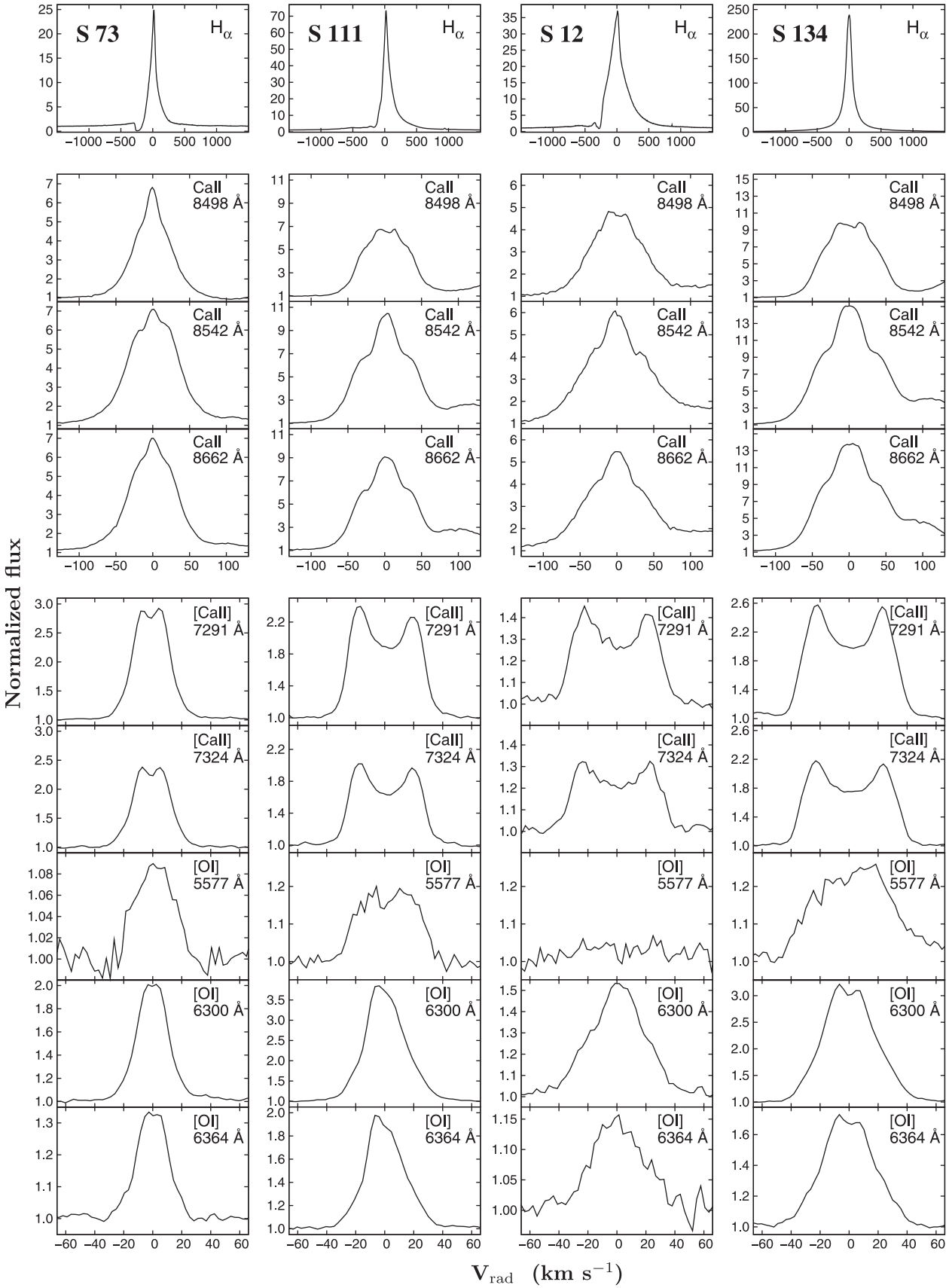

Figure 2. Same as Fig. 1 but for stars with intermediate orientation.

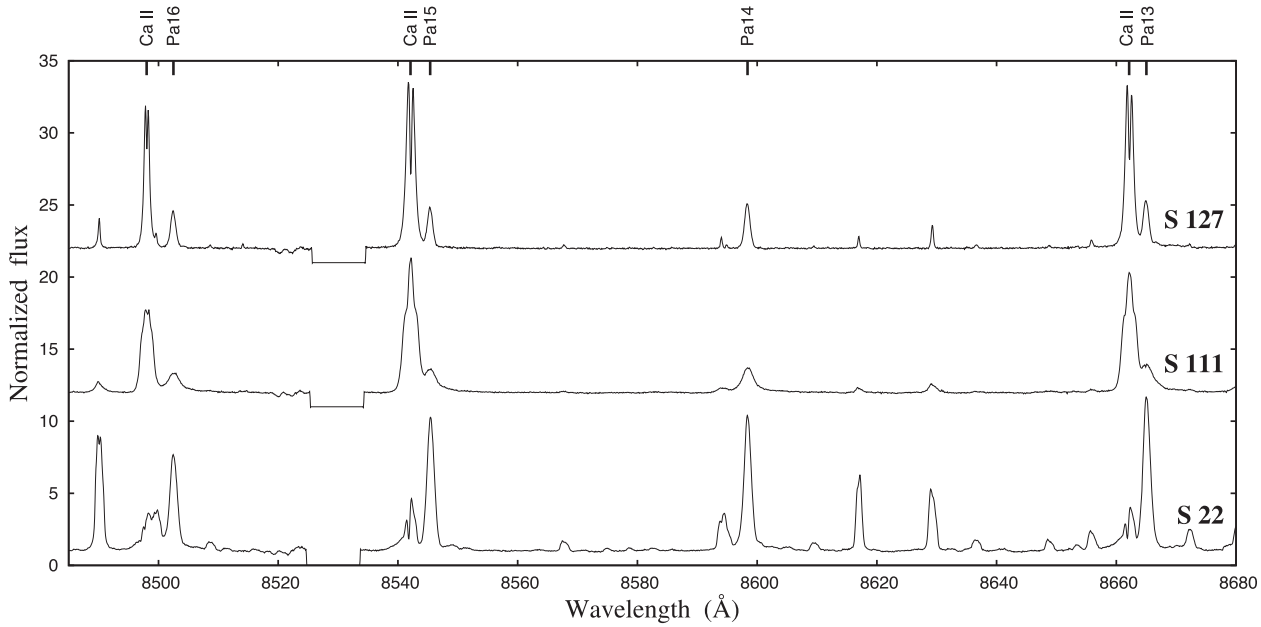

Figure 3. Ca II infrared triplet in LHA 120-S 22, LHA 120-S 111 and LHA 120-S 127. The spectra of LHA 120-S 111 and LHA 120-S 127 were shifted upwards for better viewing (by 11 and 21, respectively). The gap around 8530 Å is a short wavelength region that is not covered by the red orders of FEROS.

Table 3. Shapes and peak separations (km s^{-1}) of forbidden calcium and oxygen lines.

Object	[Ca II] 7291 Å		[Ca II] 7324 Å		[O I] 5577 Å		[O I] 6300 Å		[O I] 6364 Å	
	Shape	Separation	Shape	Separation	Shape	Separation	Shape	Separation	Shape	Separation
LHA 115-S 18	Double	10	Double	10	Single	–	Single	–	Single	–
LHA 115-S 65	Double	38	Double	37	Double?	–	Double	n. r.[a]	Double	8
LHA 120-S 12	Double	42	Double	45	No line	–	Single	–	Single?	–
LHA 120-S 22	Double	30	Double	30	Double	20	Double	13	Double	14
LHA 120-S 73	Double	11	Double	12	Single	–	Double	6	Double	6
LHA 120-S 111	Double	36	Double	36	Double?	–	Double	n. r.	Double	n. r.
LHA 120-S 127	Single	–	Single	–	Single	–	Single	–	Single	–
LHA 120-S 134	Double	45	Double	46	Broad single?	–	Double	13	Double	13

[a]n. r. – not resolved.

allows us to draw some (though preliminary) conclusions about the possible disc kinematics and density structure of the sample stars.

As was recently shown by Kraus et al. (2007, 2010), the [O I] λ5577 line arises from regions of much higher density and hence closer to the star than the [O I] λλ6300, 6364 lines. Thus, besides information on temperature and density this set of lines provides details on the kinematics within the two line-forming regions. For the B[e]SG star LHA 115-S 65 which is viewed edge-on the [O I] λ5577 line is broader than the other two [O I] lines and with stronger indication of a double-peaked profile. Simultaneous modelling of the [O I] line profiles and line luminosities led to the conclusion that the disc around LHA 115-S 65 is detached from the star and is in Keplerian rotation (Kraus et al. 2010). Furthermore, this detached disc or ring has a rather small outflow velocity which decreases with distance from the star. These findings are in strict contrast to the general belief that B[e]SG star discs are the high-density equatorial outflow parts within the two-component wind scenario of Zickgraf et al. (1985).

Comparison of the [O I] line profiles for all our sample stars indicates that the λ5577 line is indeed almost always the broadest one suggesting that Keplerian rotation rather than outflow might hold for all B[e]SG discs. Exceptions are the stars LHA 120-S 127 which is viewed exactly pole-on so that all [O I] lines are equally broad and LHA 120-S 12 for which the [O I] λ5577 line could not be detected. If the discs around the B[e]SGs are indeed in Keplerian rotation, the broader and clearly double-peaked line profiles of the [Ca II] lines must originate from regions closer to the star than the [O I] λ5577 line-forming region. Consequently, the density in the [Ca II] line-forming region must be higher.

Recently, Hartigan et al. (2004) investigated the [Ca II] λ7291/7324 line ratios in both the low- and the high-density limit and found that the ratio changes only a little from 1.495 in the former to 1.535 in the latter. They suggested the critical electron density to be of the order of $\sim 5 \times 10^7$ cm^{-3}. To obtain the [Ca II] λ7291/7324 flux ratio, we measured the equivalent widths of the lines. We supposed that the real flux ratio does not differ substantially from the measured ratio of the equivalent widths because the lines have a separation of only 30 Å. To confirm this, we checked the influence of the different continuum strengths and the effect of dereddening due to interstellar extinction by applying Kurucz model atmospheres and using the extinction values from the literature as given in Table 1. We found that for all our stars corrections to the measured equivalent width ratios are less than 1 per cent. The final values for the [Ca II] λ7291/7324 line ratios range from 1.33 to 1.47.

Table 4. Shapes and peak separations (km s^{-1}) of the Ca II infrared triplet.

Object	Ca II 8498 Å		Ca II 8542 Å		Ca II 8662 Å	
	Shape	Separation	Shape	Separation	Shape	Separation
LHA 115-S 18	Double	n. r.[a]	Double	23	Double	19
LHA 115-S 65	double	33	Double	26	Double	31
LHA 120-S 12	Multi	–	Triple	–	Triple	–
LHA 120-S 22	Multi	–	Double	28	Double	28
LHA 120-S 73	Triple	–	Triple	–	Triple	–
LHA 120-S 111	Multi	–	Triple	–	Triple	–
LHA 120-S 127	Double	16	Double	17	Double	25
LHA 120-S 134	Multi	–	Triple	–	Triple	–

[a]n. r. – not resolved.

All these values fall below the value of 1.495 for the low-density limit found by Hartigan et al. (2004). Thus, we cannot determine the electron density in the [Ca II] line-forming region from the observed flux ratios. Instead, we may use the values found within the [O I] λ5577 line-forming region as lower limits for the electron densities within the [Ca II] line-forming regions. However, so far proper density determinations within the [O I] line-forming regions have been performed for only one object, namely LHA 115-S 65 (Kraus et al. 2010).

The SMC star LHA 115-S 65 was reported to be viewed edge-on (Zickgraf et al. 1986; Kraus et al. 2010). Its [Ca II] lines are much broader than the [O I] lines and clearly double peaked. The electron density within the [O I] λ5577 line-forming region was found to be $n_e \simeq 9 \times 10^6$ cm^{-3} (Kraus et al. 2010). The range in rotational velocities over which the [Ca II] lines seem to be formed spreads from about 52 km s^{-1} as measured from the extent of the line wings to about 19 km s^{-1} as obtained from the peak separation of their profiles. Current studies of the evolutionary link of B[e]SGs to other phases in massive star evolution indicate that they could be evolving back bluewards, which means that they are in a post-red supergiant (post-RSG) or post-yellow hypergiant (post-YHG) phase (Muratore et al. 2010; Muratore et al., in preparation). Applying Keplerian rotation for the stellar mass obtained for such a scenario and given in Table 5, we find that the velocity of 52 km s^{-1} corresponds to a distance of about 22 R_* and the velocity of 19 km s^{-1} to about 160 R_*. Thus, most of the emission originates from the disc regions at roughly 160 R_*. If we assume that the disc has formed from stellar mass-loss, then its radial density structure has an r^{-2} distribution according to the law of mass conservation. Consequently, the density increases by a factor of $\gtrsim$50 over the [Ca II] emission region (from the outer to the inner edge) and becomes (much) higher than the critical density, meaning that we are in the high-density regime of the [Ca II] line formation.

The rather large range in density might be one reason why the values of the [Ca II] flux ratios do not agree with either of the limiting values computed by Hartigan et al. (2004). However, it should be noted that their values have been determined under the assumption that the material is ionized and free electrons are the dominant collision partners. Such a scenario does not hold for the discs of the B[e]SGs. Instead, the hydrogen ionization fractions were found to be very small within the [O I] line-forming regions (but still delivering an electron density higher than the critical density for [Ca II]). The discs around B[e]SGs can thus be considered as being predominantly neutral in hydrogen (Kraus et al. 2007, 2010). Hence, collisions with hydrogen atoms certainly dominate collisions with free electrons and need to be considered together with a proper radiation transfer in the lines of the infrared triplet. A proper modelling of the Ca II atom is beyond the scope of the current work. Nevertheless, we may claim that the [Ca II] lines provide a new important and appropriate tracer for the structure and kinematics of B[e]SG star discs.

3.3 Masses of B[e]SGs – their evolutionary phase

The mass of LHA 115-S 65 used for the determination of the distance of and the density within the [Ca II] line-forming region was obtained considering that the star is evolving bluewards in the Hertzsprung–Russell diagram (HRD). In such a scenario, it could

Table 5. Stellar masses, Keplerian rotation velocities and inclination angles as estimated from the [Ca II] line profiles. Values of the disc mass fluxes, f_d, are taken from Zickgraf (1998).

Object	M_{ZAMS} ($M_\odot$)	$M_{current}$ ($M_\odot$)	R_* ($R_\odot$)	$f_d/f_{d(S65)}$	r([Ca II]) (R_*)	$v_{Kep}(r)$ (km s^{-1})	v_{los} (km s^{-1})	$r(v_{Kep} = v_{los})$ (R_*)	Suggested i (°)
LHA 115-S 18	29 ± 2	19 ± 3	33 ± 3	2.15	235	21.7 ± 2.7	5	4491 ± 1104	13.5 ± 2
LHA 115-S 65	35 ± 1	25 ± 1	82	1.00	160	19.0 ± 0.4	19	161 ± 7	84 ± 6
LHA 120-S 12	22 ± 2	14 ± 2	30	2.15	235	19.8 ± 1.0	21–22.5	191 ± 41	∼90
LHA 120-S 22	41 ± 4	25 ± 4	49 ± 11	3.85	314	18.0 ± 3.5	15	469 ± 173	67 ± 23
–	49 ± 4[a]	41 ± 4	–	–	–	23.1 ± 3.7	–	763 ± 240	42 ± 8
LHA 120-S 73	25 ± 1	15 ± 1	125	0.78	141	12.7 ± 0.4	6	634 ± 42	28 ± 1
LHA 120-S 111	60 ± 5	40 ± 5	147	Unknown	–	–	18	171 ± 12	–
–	60 ± 5[a]	48 ± 5	–	–	–	–	–	192 ± 20	–
LHA 120-S 127	≥60	Unknown	75	1.31	183	–	Unresolved	–	∼0
LHA 120-S 134	42 ± 1	26 ± 1	44	2.46	251	21.2 ± 0.5	23	196 ± 8	∼90
–	50 ± 2[a]	42 ± 2	–	–	–	26.9 ± 0.6	–	344 ± 16	59 ± 2

[a]assuming that the star has just left the main sequence.

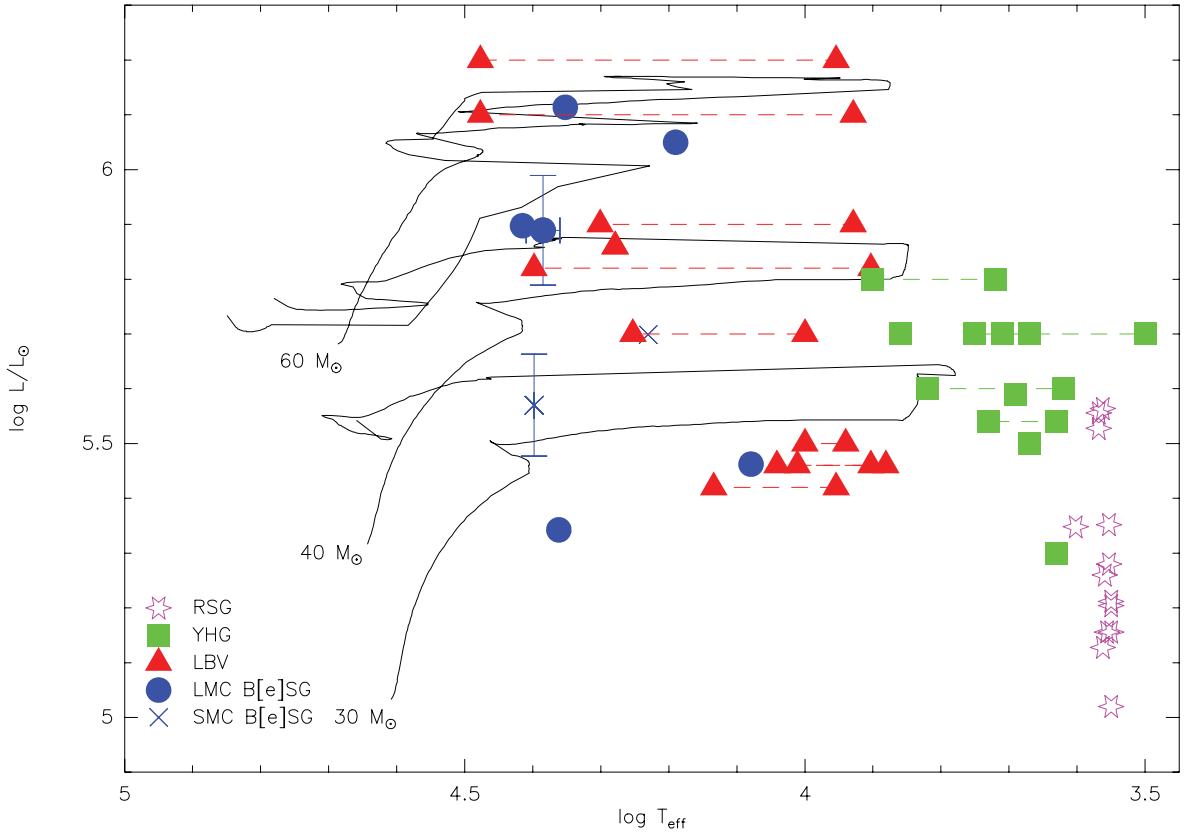

Figure 4. Our B[e]SG sample in comparison to other massive post-main-sequence phases. Stellar parameters are taken from Humphreys & Davidson (1994) and Groh et al. (2009) for the LBVs, from de Jager (1998) for the YHGs and from Levesque et al. (2005) for the RSGs. Stellar evolutionary tracks for rotating stars at LMC metallicity from Meynet & Maeder (2005) are overplotted.

have lost the mass that is now forming its disc during the passage through an RSG and/or YHG phase (see Fig. 4). So far, not much is known about the real evolutionary phase of B[e]SGs and several suggestions about their present stage can be found in the literature. For instance, it has been suggested that B[e]SGs are the results of massive binary mergers (Langer & Heger 1998; Podsiadlowski, Morris & Ivanova 2006). As of now such a scenario seems to hold for only one object, the SMC stars R4. However, one should avoid associating all B[e]SGs with stellar mergers, because the spectral characteristics of R4, its position in the HRD just at the end of the main sequence and its strong photometric variability, which is not common for B[e]SGs, displace R4 from the rest of the B[e]SG sample. We therefore consider the merger scenario as the least likely common origin for the B[e] phenomenon in the supergiant stars.

Some B[e]SGs were suggested to be evolutionary linked to luminous blue variables (LBVs) with which they share about the same region in the HRD (see Fig. 4). For instance, the star V39 in the low-metallicity galaxy IC 1613 was classified by Herrero et al. (2010) as either a B[e]SG or an LBV candidate, and the B[e]SG star LHA 115-S 65 was classified by Kraus et al. (2010) as a pre-LBV. The LBVs are luminous objects ($\log L/L_{\odot} \geq 5.4$). They were found to separate into two groups, and this separation happens at $\log L/L_{\odot} \approx 5.8$. While the more luminous LBVs were suggested to be post-main-sequence stars evolving redwards, their lower luminosity counterparts are thought to evolve bluewards, i.e. they are suggested to be post-RSGs or post-YHGs (Humphreys & Davidson 1994; Meynet et al. 2011, see also Fig. 4).

Half of our objects certainly fall into this low-luminosity regime, while two others are just at the border, but could still fit to the same scenario because their location in the HRD indicates that they might have evolved from a 40–42 $M_{\odot}$ progenitor star, which is about the limiting mass between the two evolutionary scenarios for LBVs described by Meynet et al. (2011). The possible classification of at least one of our sample B[e]SGs as a pre-LBV further suggests that the blueward evolution in this low-luminosity regime could indeed go from the YHG over the B[e]SG to the LBV phase.

In recent investigations, Kastner et al. (2010) studied the dusty discs of the Magellanic Cloud B[e]SGs. They found convincing analogues to the discs around lower mass stars in a post-asymptotic giant branch phase, so they concluded that the B[e]SGs are most likely the more massive counterparts in a post-RSG (or post-YHG) phase. And further support for such a scenario comes from recent investigations of the ^{13}C footprint for the two least massive B[e]SGs in our sample (LHA 120-S 73 and LHA 120-S 12) revealing that a post-YHG scenario is most likely for LHA 120-S 73 (Muratore et al. 2010). The $^{12}C/^{13}C$ ratio found for LHA 120-S 12 was in agreement only with an evolved nature of the star. Whether LHA 120-S 12 could also be in a post-YHG phase needs to be tested based on predictions of the $^{12}C/^{13}C$ ratio from evolutionary models for rotating stars at LMC metallicity extending to lower initial masses than provided by the current models of Meynet & Maeder (2005), but such models are not yet available.

However, a post-YHG scenario certainly fails for the most luminous B[e]SGs, for which no YHG phase exists. At which stage in

the evolution they might be (just leaving the main sequence as was suggested for the most luminous LBVs or on a blue loop) is not known.

3.4 Disc inclination angles

We now return to the [Ca II] lines. The measured peak separation of their line profiles (see Table 3) can be used to estimate possible ranges in disc inclination angles. For this, we need to know the appropriate distance from the stars at which the bulk of the [Ca II] lines form. For LHA 115-S 65 we found that this distance is about $160\,R_*$. The density reached at that distance should be very similar for the [Ca II] line-forming region for all B[e]SGs. We can estimate these distances based on the disc mass fluxes that were determined by Zickgraf (1998) for all our sample stars but LHA 120-S 111. Both the ratios of the disc mass fluxes of the sample stars with respect to LHA 115-S 65 and the resulting distances at which the required density is reached are given in Table 5.

With the obtained distances, inclination angles can be estimated from the measured peak separations together with the assumption of a Keplerian rotation law. To calculate Keplerian rotation velocities the current stellar masses need to be known. In Fig. 4, we show the positions of our objects in the HRD together with evolutionary tracks from Meynet & Maeder (2005) computed for rotating stars at LMC metallicity. The evolutionary tracks for SMC metallicity do not differ substantially from those for the LMC, so we refrain from plotting both sets of tracks. As discussed in the previous section, the B[e]SGs with $\log L/\mathrm{L}_\odot \lesssim 5.8$ might be in a post-YHG phase, while for the most luminous ones it is not clear whether they are evolving to the red or to the blue side of the HRD.

Assuming that B[e]SGs are evolving bluewards and interpolating the available evolutionary tracks, we obtained zero-age main sequence (ZAMS) and current masses for all objects as listed in Table 5. For the most massive stars in the sample we also list current masses obtained under the assumption that these stars might just have evolved off the main sequence. The stellar radii have been obtained from the temperature and luminosity values given in Table 1.

The line-of-sight velocities, $v_{\rm los}$, result from the peak separations of the [Ca II] lines. If all stars were seen edge-on, these velocities would correspond to the Keplerian velocities. To get an idea about maximum distances of the [Ca II] line-forming regions from the central stars we calculated the radial distances resulting from the peak-separation velocities. These values are listed in Table 5 in terms of stellar radii. Obviously, these distances are quite large for those stars that are considered to be seen more or less pole-on like, e.g., LHA 115-S 18.

We computed the Keplerian rotation velocities for all objects at the distance r([Ca II]) where the bulk of the [Ca II] line emission is thought to originate. From the ratio of the observed rotational velocity projected to the line of sight and the expected rotational velocity, we obtained a range in inclination angles. These values are included in Table 5. Good agreement with formerly suggested orientations is achieved for most objects. In particular, the stars LHA 115-S 18 and LHA 120-S 73 are found to be $\pm$pole-on.

The inclination angle of LHA 120-S 111 has not yet been determined. The position of this star in the HRD shows that it belongs to the most luminous objects. The masses estimated for both evolutionary scenarios can only be considered as rough estimates, and the missing value of its disc mass flux hampers a proper inclination determination. Nevertheless, considering the mass ranges as listed in Table 5, maximum distances of the [Ca II] line-forming region as obtained for a possible edge-on orientation are only slightly larger than the one obtained for LHA 115-S 65. The line strengths of the [O I] and [Ca II] lines are comparable to those of the other B[e]SGs, so that its disc mass flux should not be considerably smaller compared to LHA 115-S 65. Hence, we might conclude that LHA 120-S 111 could be oriented close to edge-on.

The values obtained for the B[e]SGs at the border between low- and high-luminosity regimes, LHA 120-S 22 and LHA 120-S 134, differ significantly for the two different evolutionary scenarios; while a close-to edge-on orientation is obtained for the post-YHG scenario, an intermediate inclination angle is obtained for the redward evolutionary scenario.

For LHA 120-S 134, both results clearly disagree with the pole-on orientation (see Table 1) as suggested by Zickgraf et al. (1986). The broad and clearly double-peaked line profiles of its [Ca II] lines definitely speak against a pole-on orientation (see Fig. 2). Which scenario will turn out to be the correct one needs further detailed investigation.

The orientation of LHA 120-S 22 in the redward evolutionary scenario delivered a value of only $i \simeq 42 \pm 8^\circ$. But this object has been reported to be viewed edge-on (Zickgraf et al. 1986). This orientation has been confirmed by Chu et al. (2003) who discovered a reflection nebula in the vicinity of LHA 120-S 22 that mirrors different viewing angles. Interestingly, a (close-to) edge-on orientation is found in the post-YHG scenario.

Inspection of the line profiles of LHA 120-S 22 reveals that this object has another peculiarity: both sets of forbidden lines are double peaked and clearly asymmetric. But while the [Ca II] lines show a much stronger red peak, the [O I] lines display a stronger blue peak. Considering that the [Ca II] lines are supposed to originate from distances closer to the star than the [O I] lines, this behaviour indicates the presence of inhomogeneities in the circumstellar material like a density wave in the disc or a spiral arm-like structure. Such structures have recently been seen on images of the disc of a young stellar object.[1] So, LHA 120-S 22 might be the first B[e]SG star with spiral arms. In any case, it is worth studying both the kinematics of its circumstellar material and the time variability of the line profiles in more detail.

We would like to emphasize that the inclination angles listed in Table 5 can only be considered as rough estimates, because several assumptions have been made for their derivation. The one with the highest uncertainty is the distance at which the [Ca II] line emission forms, because we implicitly adopt that the ionization fraction found for LHA 115-S 65 is the same in all B[e]SG star discs. This must not be true. A higher value for the ionization fraction implies a higher electron density, and the distance at which the [Ca II] emission forms is shifted farther out. The Keplerian rotation velocities are lower there and consequently the inclination of the disc would be larger. Proper values for the ionization fractions in the discs of all B[e]SGs are therefore needed. This emphasizes the need of flux calibrated data for all the sample stars.

4 CONCLUSIONS

We report on the discovery of the [Ca II] $\lambda\lambda$7291, 7324 lines in the high-resolution spectra of a sample of B[e]SGs. These lines originate from different regions than the already well-known disc tracers, the [O I] lines. The [Ca II] lines trace regions of higher density and

[1] http://www.nasa.gov/topics/universe/features/possible-planets.html

thus must form closer to the star. The combination of the kinematical information obtained from the line profiles of the [O I] and [Ca II] allows us to suggest that the material around the B[e]SGs is in Keplerian rotation. We estimated disc inclinations which are in reasonably good agreement with former guesses. However, the clearly asymmetric line profiles seen in the spectra of the star LHA 120-S 22 indicate that the material is not in a disc- or ring-like structure. We suggest that this star might have a spiral arm seen edge-on.

In addition, we discuss plausible evolutionary phases for the B[e]SGs. Although perhaps for some individual B[e]SGs (like R4 in the SMC) a different scenario might hold, a blueward evolution of (most of) the B[e]SGs seems to be likely. As suggested by Kraus (2009) and proven by Liermann et al. (2010) and Muratore et al. (2010), the ^{13}C footprint is a powerful tool to determine the evolutionary phase of B[e]SGs. Hence reliable data of the ^{13}C footprint for all B[e]SGs are needed, and we recently started an observational campaign to study the ^{13}C enrichment in the discs of all B[e]SGs. Results from these observations will certainly provide a better basis for a more detailed discussion about the evolutionary phase of B[e]SGs and their possible links to other evolved phases of massive star evolution.

ACKNOWLEDGMENTS

AA and MK acknowledge financial support from GA ČR under grant numbers 205/08/0003 and 209/11/1198. This work was supported by the research project SF0060030s08 of the Estonian Ministry of Education and Research. MFM acknowledges Universidad Nacional de La Plata for the research fellowship. MBF acknowledges Conselho Nacional de Desenvolvimento Científico e Tecnológico (CNPq-Brazil) for the post-doctoral grant. MBF acknowledges Herman Hensberge for all support with FEROS data reduction.

REFERENCES

Andrillat Y., Jaschek M., Jaschek C., 1988, A&AS, 72, 129
Andrillat Y., Jaschek M., Jaschek C., 1990, A&AS, 84, 11
Bonanos A. Z. et al., 2009, AJ, 138, 1003
Bonanos A. Z. et al., 2010, AJ, 140, 416
Borges Fernandes M., de Araújo F. X., Bastos Pereira C., Codina Landaberry S. J., 2001, ApJS, 136, 747
Borges Fernandes M., Kraus M., Chesneau O., Domiciano de Souza A., de Araújo F. X., Stee P., Meilland A., 2009, A&A, 508, 309
Briot D., 1981, A&A, 103, 1
Carr J. S., 1995, Ap&SS, 224, 25
Carr J. S., Tokunaga A. T., Najita J., Shu F. H., Glassgold A. E., 1993, ApJ, 411, L37
Chandler C. J., Carlstrom J. E., Scoville N. Z., Dent W. R. F., Geballe T. R., 1993, ApJ, 412, L71
Chu Y.-H., Chen C.-H. R., Danforth C., Dunne B. C., Gruendl R. A., Nazé Y., Oey M. S., Points S. D., 2003, ApJ, 125, 2098
Curé M., 2004, ApJ, 614, 929
Curé M., Rial D. F., Cidale L., 2005, A&A, 437, 929
de Jager C., 1998, A&AR, 8, 145
Groh J. H. et al., 2009, ApJ, 705, L25
Hamann F., 1984, ApJS, 93, 485
Hamann F., Persson S. E., 1992a, ApJS, 82, 247
Hamann F., Persson S. E., 1992b, ApJS, 82, 285
Hartigan P., Edwards S., Pierson R., 2004, ApJ, 609, 261
Herrero A., Garcia M., Uytterhoeven K., Najarro F., Lennon D. J., Vink J. S., Castro N., 2010, A&A, 513, A70
Humphreys R. M., Davidson K., 1994, PASP, 106, 1025
Ignace R., Brimeyer A., 2006, MNRAS, 371, 343
Jaschek C., Andrillat Y., Jaschek M., Egret D., 1988, A&A, 192, 285
Kastner J. H., Buchanan C., Sahai R., Forrest W. J., Sargent B. A., 2010, AJ, 139, 1993
Kraus M., 2006, A&A, 456, 151
Kraus M., 2009, A&A, 494, 253
Kraus M., Borges Fernandes M., 2005, in Ignace R., Gayley K. G., eds, ASP Conf. Ser. Vol. 337, The Nature and Evolution of Disks Around Hot Stars. Astron. Soc. Pac., San Francisco, p. 254
Kraus M., Krügel E., Thum C., Geballe T. R., 2000, A&A, 362, 158
Kraus M., Borges Fernandes M., Kubát J., de Araújo F. X., Lamers H. J. G. L. M., 2005, A&A, 441, 289
Kraus M., Borges Fernandes M., de Araújo F. X., 2007, A&A, 463, 627
Kraus M., Borges Fernandes M., de Araújo F. X., 2010, A&A, 517, A30
Kwan J., Fischer W., 2011, MNRAS, 411, 2383
Lamers H. J. G. L. M., Pauldrach A. W. A., 1991, A&A, 244, L5
Langer N., Heger A., 1998, in Hubert A. M., Jaschek C., eds, Astrophysics and Space Science Library, Vol. 233, B[e] Stars. Kluwer, Dordrecht, p. 235
Levesque E. M., Massey P., Olsen K. A. G., Plez B., Josselin E., Maeder A., Meynet G., 2005, ApJ, 628, 973
Liermann A., Kraus M., Schnurr O., Borges Fernandes M., 2010, MNRAS, 408, L6
Magalhães A. M., 1992, ApJ, 398, 286
Magalhães A. M., Melgarejo R., Pereyra A., Carciofi A. C., 2006, in Kraus M., Miroshnichenko A. S., eds, ASP Conf. Ser. Vol. 355, Stars with the B[e] Phenomenon. Astron. Soc. Pac., San Francisco, p. 147
McGregor P. J., Hillier D. J., Hyland A. R., 1988, ApJ, 334, 639
Melgarejo R., Magalhães A. M., Carciofi A. C., Rodrigues C. V., 2001, A&A, 377, 581
Meynet G., Maeder A., 2005, A&A, 429, 581
Meynet G., Georgy C., Hirschi R., Maeder A., Massey P., Przybilla N., Nieva M.-F., 2011, Bull. Soc. R. Sci. Liege, 80, 266
Morris P. W., Eenens P. R. J., Hanson M. M., Conti P. S., Blum R. D., 1996, ApJ, 470, 597
Muratore M. F., Kraus M., Liermann A., Schnurr O., Cidale L. S., Arias M. L., 2010, Bol. Asociación Argentina Astron., 53, 123
Najita J., Carr J. S., Glassgold A. E., Shu F. H., Tokunaga A. T., 1996, ApJ, 462, 919
Osterbrock D. E., 1989, Astrophysics of Gaseous Nebulae and Active Galactic Nuclei. University Science Books, Sausalito, CA
Oudmaijer R. D., Drew J. E., 1999, MNRAS, 305, 166
Pelupessy I., Lamers H. J. G. L. M., Vink J. S., 2000, A&A, 359, 695
Podsiadlowski Ph., Morris T. S., Ivanova N., 2006, in Kraus M., Miroshnichenko A. S., eds, ASP Conf. Ser. Vol. 355, Stars with the B[e] Phenmenon. Astron. Soc. Pac., San Francisco, p. 259
Polidan R. S., Peters G. J., 1976, in Slettebak A., ed., Proc. IAU Symp. 70, Be and Shell Stars. Reidel Publishing Company, Dordrecht, p. 59
Verschueren W., Brown A. G. A., Hensberge H., David M., Le Poole R. S., de Geus E. J., de Zeeuw P. T., 1997, PASP, 109, 868
Zickgraf F.-J., 1998, Habilitation Thesis, Univ. Heidelberg
Zickgraf F.-J., Wolf B., Stahl O., Leitherer C., Klare G., 1985, A&A, 143, 421
Zickgraf F.-J., Wolf B., Leitherer C., Appenzeller I., Stahl O., 1986, A&A, 163, 119
Zickgraf F.-J., Wolf B., Stahl O., Humphreys R. M., 1989, A&A, 220, 206

This paper has been typeset from a TEX/LATEX file prepared by the author.